Acta Ophthalmologica

Acta Ophthalmologica 2015

Assessment of parafoveal cone density in patients taking hydroxychloroquine in the absence of clinically documented retinal toxicity

Guillaume Debellemanière, Mathieu Flores, Perle Tumahai, Mathieu Meillat, Mélanie Bidaut Garnier, Bernard Delbosc and Maher Saleh

Department of Ophthalmology, Besançon University Hospital, University of Franche-Comté, Besançon, France

ABSTRACT.

Purpose: **To measure cone density in patients taking hydroxychloroquine (HCQ), with no clinical evidence of maculopathy.**

Methods: **Patients visiting for HCQ macular toxicity screening in the Besançon University Hospital Ophthalmology Department (France) were studied. They underwent routine examination including spectral-domain optical coherence tomography, fundus autofluorescence and multifocal electroretinogram to detect HCQ-induced retinal toxicity. Cone metrics (density, spacing and percentage of cones with six neighbours) were obtained using an adaptive optics camera (RTX1, Imagine Eyes, Orsay, France). The region of interest corresponded to a 0.3° × 0.3° square placed nasally and temporally at 2° of eccentricity from the fovea.**

Results: **Forty eyes of 23 patients were studied. The majority of the patients (21/23) were female. They were aged from 25 to 60 years (mean age ± SD: 40.1 years ± 10). The cumulative dose for HCQ ranged from 24 to 2160 g (777 ± 558 g). None of them displayed HCQ toxicity on screening tests. Bivariate analysis showed moderate cone loss with escalating doses of HCQ (linear regression, $r^2 = 0.23$, $p = 0.018$). Cone spacing also increased with increasing cumulative dose ($r^2 = 0.17$, $p = 0.008$). Cone packing remained unchanged ($p > 0.05$). Multivariate analysis showed that age and cumulative dose were additive and independent factors of cone dropout.**

Conclusions: **In this pilot study, we observed moderate cone loss as HCQ cumulative doses increased. The early detection of parafoveal cone metric changes may represent the earliest sign of HCQ macular toxicity during screening.**

Key words: cone density – hydroxychloroquine toxicity – retinal imaging – screening

Acta Ophthalmol. 2015: 93: e534–e540

© 2015 Acta Ophthalmologica Scandinavica Foundation. Published by John Wiley & Sons Ltd

doi: 10.1111/aos.12728

Introduction

Long-term administration of chloroquine (CQ) or hydroxychloroquine (HCQ) can be responsible for progressive and rapidly irreversible retinal toxicity, with dramatic visual prognosis if not detected early (Cambiaggi 1957; Hobbs et al. 1959). Screening procedures recommended by the American Academy of Ophthalmology include measurement of best-corrected visual acuity (BCVA), slit lamp and dilated fundus examination, automated threshold visual field (VF) testing with a white 10-2 pattern and ideally at least one of the following: spectral-domain optical coherence tomography (SD-OCT), fundus autofluorescence (FAF) and multifocal electroretinogram (mfERG) (Marmor et al. 2011). Considering that retinal pigment epithelium alteration is preceded by photoreceptor modifications (Rosenthal et al. 1978), the detection of cone metric changes in the parafoveal area could provide earlier and more sensitive detection of beginning toxicity. Adaptive optics (AO) retinal imaging, which uses active optical elements to compensate optical aberrations of the eye, provides direct visualization of the living retina. Adaptive optics has already proven its utility by highlighting cone changes in a variety of retinal diseases (Wolfing et al. 2006; Boretsky et al. 2012; Hansen et al. 2013; Tojo et al. 2013a,b; Yokota et al. 2013; Bek 2014; Saleh et al. 2014). Recently, Stepien et al. (2009) reported irregularities in the cone mosaic studied by AO in two patients presenting confirmed HCQ maculopathy. In this study, we investigated cone counts in patients with various cumulative doses of HCQ in the absence of clinically evident toxicity, to assess its potential use as a screening tool in the early course of the disease.

Materials and Methods

Screening procedure for HCQ retinopathy

Patients consulting for HCQ macular toxicity screening in the Besançon University Hospital Ophthalmology

Department (France) were included between July 2012 and May 2013. Selection criteria were intended to ensure good image quality. Therefore, patients presenting keratitis, dry eye syndrome, cataract, tear film instability, myopia or hyperopia, and/or astigmatism exceeding three dioptres, any macular disease, including previously known CQ/HCQ retinopathy, or less than 20/20 BCVA were excluded.

All patients underwent a comprehensive ophthalmological examination with BCVA measurement and indirect ophthalmoscopy. Axial lengths were measured using a biometer (IOLMaster 500; Carl Zeiss Meditec, Dublin, CA, USA). Spherical equivalent refractive errors were measured using the TONOREF II autorefractometer (Nidek, Aichi, Japan). Automated threshold VF testing was performed with a white 10-2 pattern (Octopus 900 perimeter; Haag-Streit Inc, Koeniz, Switzerland). Fundus autofluorescence (Topcon Retinal Camera TRC-50DX; Topcon Medical System, Inc., Oakland, NJ, USA) was obtained. The early finding of a pericentral ring of increased FAF or the more advanced stage of speckled or coalescent dark areas was sought. A mfERG (Vision Monitor; Metrovision, Pérenchies, France) was recorded according to the International Society for Clinical Electrophysiology of Visioncriteria by an experienced technician. Several methods of mfERG analysis were described in the evaluation of HCQ retinal toxicity (Lyons & Severns 2007; Graves et al. 2014). Ring ratio analysis was used in our study for its good sensitivity, specificity and reproducibility. SD-OCT was performed using the Spectralis OCT (Heidelberg Engineering, Dossenheim, Germany). The protocol consisted of 19 horizontal sections of 20° length with 1024 A-scans/B-scans. At least nine B-scans per image were averaged by the Tracking Automatic Real-Time software. Perifoveal loss of the photoreceptor ellipsoid band and outer nuclear atrophy was sought.

Visual field, mfERG, FAF and SD-OCT signs of CQ or HCQ retinal toxicity were determined by two study investigators (GD and MF), in a blind manner regarding the other investigator's grade.

Adaptive optics imaging

At the same visit, all patients were examined using an AO commercial prototype (RTX-1®; Imagine Eyes™, Orsay, France). This camera is based on a non-coherent flood-illuminated design with an 850-nm central illumination wavelength with a $4° \times 4°$ imaging field of view allowing high-resolution imaging of macular cones with a lateral resolution of 2 μm. Its low-noise CCD camera has a 1.6-μm pixel resolution and a 9.5-fps frame.

Adaptive optics imaging sessions were conducted after the pupils were dilated with one drop each of 0.5% tropicamide. The spherical ametropia was entered for spherical correction. The area of the retina to study was chosen by adjusting the position of the fixation target horizontally, and the imaging depth was chosen within the range of 0 to -80 μm to obtain the sharpest image. On the device's control panel, a numerical value informed the operator of the level of AO correction: the lower this value was the better the correction and thus the better the acquisition quality. During acquisition, which lasted on average 30 seconds per eye, 40 live high-resolution images of the retina were automatically averaged by the device.

Image processing

Each series of 40 images acquired by the AO camera was processed using software programs provided by the system manufacturer (ck v0.1 and AOdetect v0.1; Imagine Eyes). These images were recorded using a cross-correlation method (Zitova & Flusser 2003) and averaged to produce a final image with an improved signal-to-noise ratio. The raw images that showed artefacts due to eye blinking and saccades were automatically eliminated before averaging. For display and printing purposes, the background of the resulting image was subtracted using a Gaussian filter and the histogram was stretched over a 16-bit range of grey levels.

The positions of photoreceptors were computed by automatically detecting the central co-ordinates of small circular spots whose brightness was higher than the surrounding background level. First, the averaged image, as obtained before background removal and histogram stretching, was further processed using adaptive (Kuan et al. 1985) and multiple-scale (Lindeberg 1994) digital filters. Then, the local maxima of the resulting filtered image were detected and their pixel co-ordinates were recorded. The spatial distribution of these point co-ordinates was finally analysed in terms of intercell spacing, local cell density and the number of nearest neighbours using Delaunay triangulation (De Berg et al. 2008a) and Voronoi diagrams (De Berg et al. 2008b).

As the foveola itself is not properly seen with the RTX-1 device due to limited resolution in the very centre, two $0.3° \times 0.3°$ squares were placed where the cone density was found to be maximal, nasally and temporally along the horizontal axis of the eye studied (Fig. 1). This recently detailed counting method (Bidaut Garnier et al. 2014) provides good reproducibility of measurements in normal volunteers in the same examination conditions. Cone spacing and the percentage of cones with six neighbours (nearest neighbour analysis) assessed on the Voronoi index were also analysed in the same area. The data presented correspond to the mean of the nasal and temporal measurements. The estimates of cone density were verified by two investigators (MS, GD) to minimize any potential cone under- or oversampling made by the automated software. Taking into account the probability of an initial asymmetric retinopathy, both eyes from each patient were studied.

Population studied

Sixty-four eyes of 32 patients were initially studied. Twenty-four eyes (37.5%) of 15 patients were excluded from the analysis because of insufficient AO image quality (defined as preprocessed images where the cone mosaic could not be identified in the region of interest by either of the two graders, whatever the magnification was). Forty eyes of 23 patients were analysed.

The patients' demographics and the results of the AO images analysis are summarized in Table 1. The majority of patients (21/23) were female. They ranged in age from 25 to 60 years (40.1 ± 10 years). The cumulative HCQ dose ranged from 24 to 2160 g (777 ± 558 g); 69.5% of the patients were treated for systemic lupus eryth-

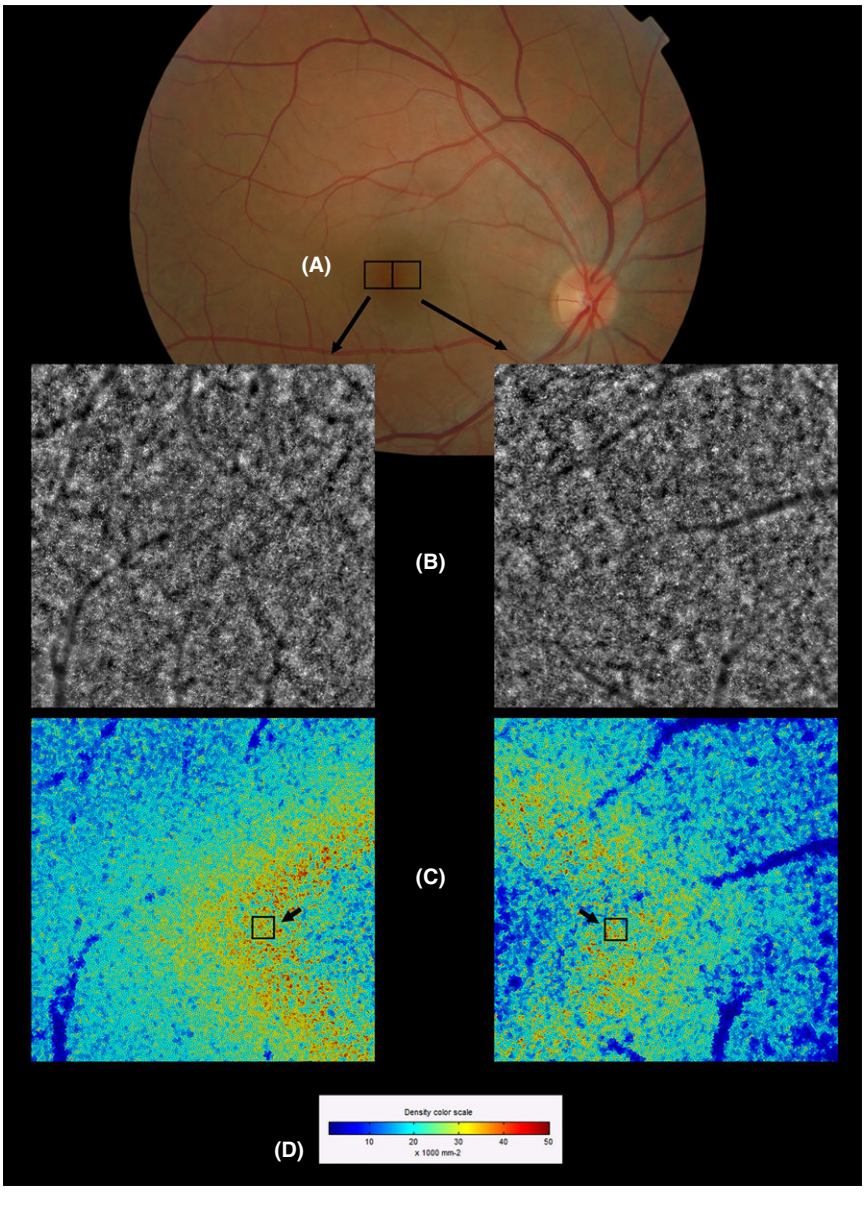

Fig. 1. Adaptive optics (AO) imaging. Two raw AO images of 4° × 4°, centred on 2° of eccentricity from the fovea (A), were acquired nasally and temporally (B). The region of interest, where the cone metrics were measured, corresponded to a 0.3° × 0.3° square. Cone densities were measured using AODetect v0.1 provided by the manufacturer (C). The results are presented according to a colour scale (D).

ematosus. None of the patients had a proven HCQ retinopathy requiring interruption of treatment. Examples of cone densities, spacing and mosaic packing in seven patients are shown in (Fig. 2).

Statistical analysis

All values represent the mean ± standard deviation. Descriptive statistics and the Mann–Whitney test were used for statistical comparison of the two groups with the two-tailed p-value ≤ 0.05 considered significant. The nonparametric correlation with calculation of the Spearman *r* was performed. Linear regression graphs were obtained using Graph Prism 6 (GraphPad Instattm, Inc., San Diego, CA, USA). The study was conducted with the approval of the local Besançon University Hospital ethics committee after informed consent had been obtained from the patients, and the study adhered to the tenets of the Declaration of Helsinki.

Results

Nasal and temporal densities were comparable (mean ± SD: 27 155 ± 2705 and 27 154 ± 2737 cells/mm², respectively).

There was a significant negative correlation between cone density and HCQ dose (r^2 = 0.23, p = 0.0018, Fig. 3) and a significant positive correlation between cone spacing and HCQ dose (r^2 = 0.17, p = 0.008, Fig. 4). No relationship was found between the cumulative dose and the regularity of the cone mosaic. Cone density decreased (r^2 = 0.17, p = 0.008, Fig. 5), and spacing increased with age (r^2 = 0.16, p = 0.01, Fig. 6). Multivariate analysis showed that age and cumulative dose were additive and independent factors of parafoveal cone density dropout (Table 2; r^2 = 37.10%, p < 0.001) and cone spacing increase (Table 3; r^2 = 30.50%, p = 0.001).

Discussion

This pilot study is the first to quantify cones using an AO camera in patients on a HCQ regimen. There was a negative correlation between parafoveal cone density and cumulative HCQ dose. This finding suggests that cone loss may occur at an early stage after exposure to HCQ, even in the absence of clinically evident toxicity.

Recently, Stepien et al. (2009) suggested that AO imaging might be the most appropriate tool to demonstrate abnormalities in the outer retina in HCQ retinopathy at a preclinical stage. They described the cases of two patients with long-term HCQ use presenting subtle perifoveal ophthalmoscopic pigmentary changes and bilateral perifoveal defects on automated Humphrey VF 10-2 perimetry. All four eyes displayed complete loss of the photoreceptor inner segment/outer segment junction, with relative preservation of the retinal pigmentary epithelium and the inner retina layers on SD-OCT. AO showed some dropout in cone counts, an increase in cone spacing and disorganization of the cone mosaic in the area corresponding to the OCT defects. In the current study, we report similar findings in patients with normal eye fundus and normal ancillary tests.

We studied cones in the parafoveal area for several reasons, the most prominent of which is that the onset of HCQ retinal toxicity usually starts in this area (Marmor et al. 2011). In

Table 1. Patient demographics and adaptive optics findings.

Patient number	Gender (M/F)	Age (years)	Cumulative dose (g)	Pathology	Eye number	RE/LE	Nasal density (cells/mm²)	Temporal density (cells/mm²)	Average density (cells/mm²)	Nasal spacing (μm)	Temporal spacing (μm)	Average spacing (μm)	Nasal NNA (%)	Temporal NNA (%)	Average NNA (%)
1	F	34	24	SLE	1	RE	23 568	25 693	24 630	7.30	6.88	7.09	44.80	42.10	43.45
					2	LE	27 737	28 404	28 071	6.55	6.61	6.58	45.70	38.80	42.25
2	F	32	48	SLE	3	RE	29 493	29 988	29 741	6.42	6.36	6.39	48.30	54.10	51.20
					4	LE	29 948	30 483	30 216	6.39	6.37	6.38	48.20	53.00	50.60
3	F	27	72	SLE	5	RE	26 317	30 374	28 346	6.81	6.33	6.57	53.40	48.50	50.95
4	F	36	72	Connective tissue disease	6	RE	30 133	28 893	29 513	6.39	6.53	6.46	50.60	43.30	46.95
					7	LE	27 643	27 157	27 400	6.68	6.75	7.29	50.70	41.60	41.30
5	F	45	126	Mouth ulcers	8	RE	27 901	27 574	27 738	6.59	6.64	6.61	45.70	34.40	40.05
					9	LE	28 193	29 891	29 042	6.55	6.44	6.49	43.40	45.80	44.60
6	F	47	288	RA	10	RE	25 285	25 021	25 153	6.95	7.01	6.98	42.70	42.10	42.40
7	F	25	288	SLE	11	RE	31 246	28 276	29 761	6.24	6.58	6.41	44.70	42.00	43.35
					12	LE	30 625	28 553	29 589	6.34	6.56	6.45	43.80	40.80	42.30
8	M	37	312	SLE	13	RE	28 740	30 112	29 426	6.53	6.36	6.45	44.00	46.80	45.40
					14	LE	31 072	29 628	30 350	6.25	6.39	6.32	50.30	49.60	49.95
9	F	32	360	SLE	15	RE	29 437	29 570	29 504	6.50	6.43	6.47	41.30	44.70	43.00
10	F	57	432	Sarcoidosis	16	RE	27 568	25 249	26 409	6.74	7.01	6.87	42.10	46.20	44.15
					17	LE	26 494	23 777	25 135	6.81	7.18	6.99	43.60	45.70	44.65
11	F	60	438	RA	18	LE	25 692	24 914	25 303	6.89	7.03	6.96	36.00	41.70	38.85
12	F	25	550	SLE	19	RE	27 943	24 905	26 424	6.60	7.03	6.81	50.10	40.50	45.30
13	F	56	720	RA	20	RE	29 157	28 527	28 842	6.47	6.54	6.51	45.80	47.00	46.40
					21	LE	27 830	28 080	27 955	6.63	6.60	6.61	44.70	44.10	44.40
14	F	45	730	SLE	22	RE	26 947	25 363	26 041	6.75	6.93	6.84	33.20	44.20	38.70
					23	LE	29 597	30 910	30 254	7.33	6.26	6.79	44.60	47.60	46.10
15	F	52	864	RA	24	RE	25 068	24 860	24 964	6.97	7.01	6.99	38.20	43.50	40.85
					25	LE	24 653	24 236	24 445	7.03	7.16	7.10	41.80	40.30	41.05
16	F	39	1008	SLE	26	RE	24 869	24 259	25 388	7.00	7.07	7.03	41.90	52.20	47.05
					27	LE	25 460	22 699	24 079	6.92	7.33	7.13	45.80	41.10	43.45
17	F	25	1095	SLE	28	RE	28 494	31 766	30 130	6.55	6.20	6.37	43.50	46.20	44.85
					29	LE	27 510	30 187	28 848	6.67	6.37	6.52	40.60	47.50	44.05
18	F	30	1468	SLE	30	RE	28 813	28 425	26 721	6.50	6.53	6.51	41.90	48.00	44.95
					31	LE	27 149	29 957	28 553	6.71	6.41	6.56	49.80	44.40	47.10
19	F	48	1600	SLE	32	RE	27 770	27 733	27 752	6.62	6.60	6.61	39.70	38.90	39.30
					33	LE	25 050	26 077	25 564	7.03	6.80	6.92	46.90	45.50	46.20
20	M	53	1679	SLE	34	RE	25 472	27 229	26 350	7.05	6.77	6.91	41.40	41.90	41.65
21	F	30	1728	SLE	35	RE	29 736	28 085	28 910	6.43	6.62	6.52	46.60	43.00	44.80
					36	LE	30 998	27 877	29 437	6.26	6.61	6.43	45.30	48.90	47.10
22	F	53	1800	SLE	37	RE	21 359	20 291	20 825	7.56	7.88	7.72	43.10	38.40	40.75
					38	LE	23 025	25 665	24 345	7.27	6.89	7.08	42.70	44.40	43.55
23	F	34	2160	SLE	39	RE	20 110	21 878	20 994	7.77	7.46	7.61	40.50	47.20	43.85
					40	LE	22 110	23 590	22 850	7.45	7.21	7.33	42.00	44.00	43.00

SLE = systemic lupus erythematosus; RA = rheumatoid arthritis; LE = left eye; RE = right eye; NNA = nearest neighbour analysis (% of cones with six neighbours).

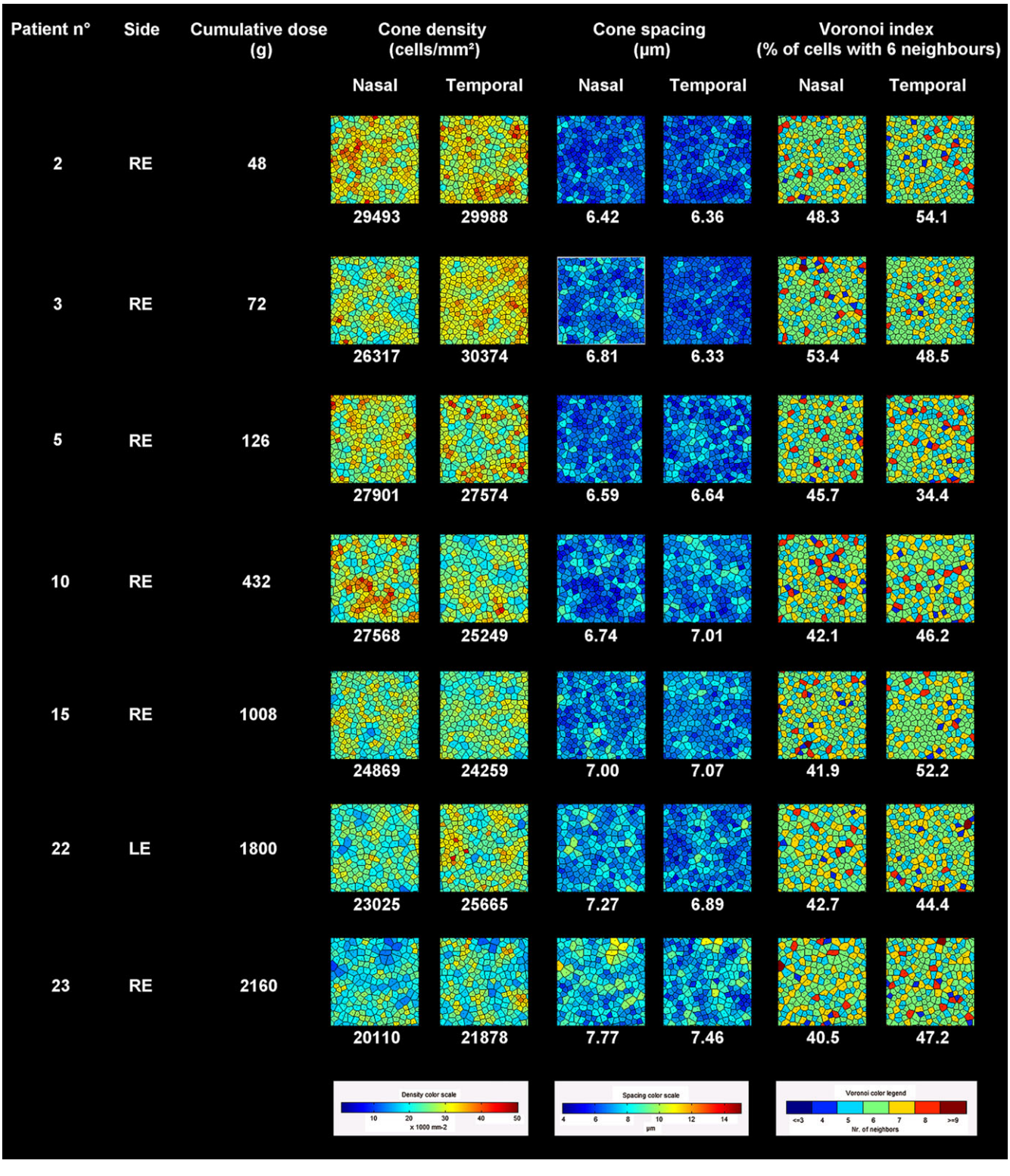

Fig. 2. Examples of cone densities, spacing and mosaic packing in seven patients with different cumulative doses of hydroxychloroquine. Cone dropout, an increase in spacing and relative conservation of the cone mosaic were noted as the cumulative dose progressively increased.

addition, due to resolution limitation of the AO camera, cones appear blurred in the very centre of the foveola. It should also be noted that at this eccentricity, cone cells still outnumber other cell contingencies (Fitzpatrick 2004), reinforcing the accuracy of the automated detection of cones by the algorithm of the software.

The limitations of this study include the relatively small sample size and its cross-sectional design. It should be also noted that we studied both eyes of patients taking a HCQ regimen, as was performed in previous studies examining HCQ toxicity (Lyons & Severns 2007; Adam et al. 2012). To the extent that one eye may not have behaved

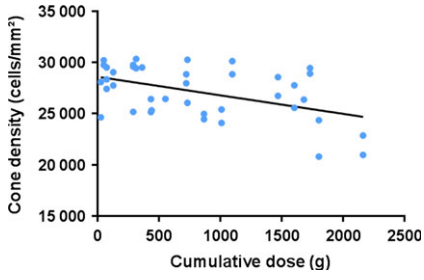

Fig. 3. Relationship between cone density and cumulative dose of hydroxychloroquine (r^2 = 0.23, p = 0.002).

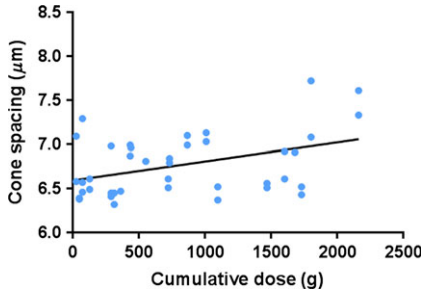

Fig. 4. Relationship between cone spacing and cumulative dose of hydroxychloroquine (r^2 = 0.17, p = 0.008).

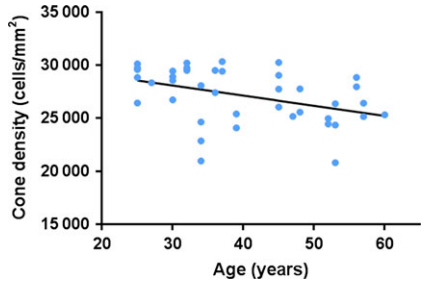

Fig. 5. Relationship between cone density and age (r^2 = 0.17, p = 0.08).

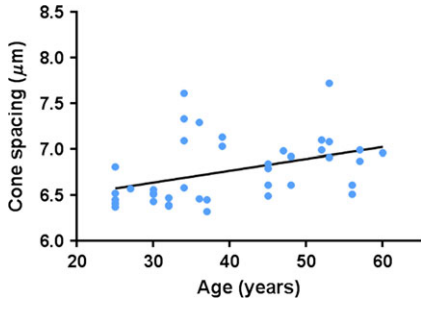

Fig. 6. Relationship between cone spacing and age (r^2 = 0.16, p = 0.01).

independently of the other, inclusion of both eyes may have magnified statistical significance, or the lack thereof.

Table 2. Results of multiple regression analysis of factors that influenced parafoveal cone density.

Variable	*t* Ratio	p Value
[A] Mean cone density (constant)	24.842	<0.0001
[B] Cumulative dose	3.426	0.0015
[C] Age	2.886	0.0065
Equation that fits the data the best	31 998−1.697 × [B]−87.526 × [C]	
r^2	37.10%	0.0002

Table 3. Results of multiple regression analysis of factors that influenced parafoveal cone spacing.

Variable	*t* Ratio	p Value
[A] Mean cone spacing (constant)	32.78	<0.0001
[B] Cumulative dose	2.766	0.0088
[C] Age	2.696	0.0105
Equation that fits the data the best	[A] = 6.131 + 0.0001989 × [B] + 0.01187 × [C]	
r^2	30.5%	0.0012

There was also a gender bias as most of our patients were females, consistent with the preponderance of autoimmune conditions in women. In addition, dry eye disease leading to tear film instability, keratitis and cataract promoted by corticosteroid therapy are common conditions in the population treated with HCQ, and their exclusion may have decreased the power of the study. It should also be noted that none of the patients included presented a proven HCQ retinopathy.

Interestingly, the only three patients with suspected toxicity (OCT-mERG and HVF defects with normal eye fundus and unremarkable FAF) had their AO images discarded from the analysis due to poor quality. Given the high number of uninterpretable images, one could conclude that AO is not yet suitable for routine screening for beginning HCQ toxicity. Even when the image is exploitable, the true disease status can only be determined by following the subjects for a period of time, possibly several years, to determine which patients ultimately develop a toxic maculopathy. Consequently, technical improvements are still needed to acquire AO images in the patients on a HCQ regimen comprehensively, especially those with media opacities. Notwithstanding these difficulties, AO appears to be a promising tool, easy to implement in daily clinical practice. Long-term follow-up taking advantage of the ability to longitudinally track disease with the AO device would certainly add valuable information on the natural history of cone survival exposed to a HCQ regimen.

Conclusions

Parafoveal cone density decreases in patients taking HCQ, even in the absence of clinical evidence of toxicity. Further studies are warranted to assess the long-term implications of these changes.

References

Adam MK, Covert DJ, Stepien KE & Han DP (2012): Quantitative assessment of the 103-hexagon multifocal electroretinogram in detection of hydroxychloroquine retinal toxicity. Br J Ophthalmol **96**: 723–729.

Bek T (2014): Fine structure in diabetic retinopathy lesions as observed by adaptive optics imaging. A qualitative study. Acta Ophthalmol **92**: 753–758.

Bidaut Garnier M, Flores M, Debellemanière G et al. (2014): Reliability of cone counts using an Adaptive Optics retinal camera. Clin Experiment Ophthalmol **42**: 833–840.

Boretsky A, Khan F, Burnett G, Hammer DX, Ferguson RD, Van Kuijk F & Motamedi M (2012): *In vivo* imaging of photoreceptor disruption associated with age-related macular degeneration: a pilot study. Lasers Surg Med **44**: 603–610.

Cambiaggi A (1957): Unusual ocular lesions in a case of systemic lupus erythematosus. Arch Ophthalmol **57**: 451–453.

De Berg M, Cheong O & van Kreveld M (2008a): Delaunay triangulation. In: De Berg M, Cheong O, van Kreveld M & Overmars M (eds). Computational geometry. 3rd edn. Berlin-Heidelberg: Springer 191–218.

De Berg M, Cheong O & van Kreveld M (2008b): Voronoi diagrams. In: De Berg M,

Cheong O, van Kreveld M & Overmars M (eds). Computational geometry. 3rd edn. Berlin-Heidelberg: Springer 147–170.

Fitzpatrick D (2004): Anatomical distribution of rods and cones. In: Purves D, Augustine GJ, Fitzpatrick D, Hall WC, LaMantia AS, McNamara JO, Mark Williams S (eds). Neuroscience, 3rd edn. Sunderland, MA: Sinauer Associates 244–245.

Graves GS, Adam MK, Stepien KE & Han DP (2014): Validation of the colour difference plot scoring system analysis of the 103 hexagon multifocal electroretinogram in the evaluation of hydroxychloroquine retinal toxicity. Acta Ophthalmol **92**: 377–381.

Hansen SO, Cooper RF, Dubra A, Carroll J & Weinberg DV (2013): Selective cone photoreceptor injury in acute macular neuroretinopathy. Retina **33**: 1650–1658.

Hobbs HE, Sorsby A & Freedman A (1959): Retinopathy following chloroquine therapy. Lancet **2**: 478–480.

Kuan DT, Sawchuk AA, Strand TC & Chavel P (1985): Adaptive noise smoothing filter for images with signal-dependent noise. IEEE Trans Pattern Anal Mach Intell **7**: 165–177.

Lindeberg T (1994). Linear scale-space and related multi-scale representations. In: Lindeberg T (ed.). Scale-space theory in computer vision. Norwell, MA, USA: Kluwer Academic Publishers 31–58.

Lyons JS & Severns ML (2007): Detection of early hydroxychloroquine retinal toxicity enhanced by ring ratio analysis of multifocal electroretinography. Am J Ophthalmol **143**: 801–809.

Marmor MF, Kellner U, Lai TYY, Lyons JS, Mieler WF & American Academy of Ophthalmology (2011): Revised recommendations on screening for chloroquine and hydroxychloroquine retinopathy. Ophthalmology **118**: 415–422.

Rosenthal AR, Kolb H, Bergsma D, Huxsoll D & Hopkins JL (1978): Chloroquine retinopathy in the rhesus monkey. Invest Ophthalmol Vis Sci **17**: 1158–1175.

Saleh M, Debellemanière G, Meillat M, Tumahai P, Bidaut Garnier M, Flores M, Schwartz C & Delbosc B (2014): Quantification of cone loss after surgery for retinal detachment involving the macula using adaptive optics. Br J Ophthalmol **98**: 1343–1348.

Stepien KE, Han DP, Schell J, Godara P, Rha J & Carroll J (2009): Spectral-domain optical coherence tomography and adaptive optics may detect hydroxychloroquine retinal toxicity before symptomatic vision loss. Trans Am Ophthalmol Soc **107**: 28–33.

Tojo N, Nakamura T, Ozaki H, Oka M, Oiwake T & Hayashi A (2013a): Analysis of macular cone photoreceptors in a case of occult macular dystrophy. Clin Ophthalmol **7**: 859–864.

Tojo N, Nakamura T, Fuchizawa C, Oiwake T & Hayashi A (2013b): Adaptive optics fundus images of cone photoreceptors in the macula of patients with retinitis pigmentosa. Clin Ophthalmol **7**: 203–210.

Wolfing JI, Chung M, Carroll J, Roorda A & Williams DR (2006): High-resolution retinal imaging of cone-rod dystrophy. Ophthalmology **113**: 1019.

Yokota S, Ooto S, Hangai M, Takayama K, Ueda-Arakawa N, Yoshihara Y, Hanebuchi M & Yoshomura N (2013): Objective assessment of foveal cone loss ratio in surgically closed macular holes using adaptive optics scanning laser ophthalmoscopy. PLoS One **8**: e63786.

Zitova B & Flusser J (2003): Image registration methods: a survey. Image Vis Comput **21**: 977–1000.

Received on November 17th, 2014.
Accepted on March 1st, 2015.

Correspondence:
Maher Saleh
Department of Ophthalmology
Besançon University Hospital
Jean Minjoz 3, Boulevard Fleming
Besançon 25030, France
Tel: +33 3 81 66 94 47
Fax: +33 3 81 66 84 75
Email: msaleh@chu-besancon.fr

This work was presented during the European Association for Vision and Eye Research (EVER) annual meeting, 20 October 2013. It won the 'section paper abstract prize'. This study was funded by the 'Franc-Comtoise Association for Research in Ophthalmology' (AFCRO).